Journal of Pathology
J Pathol 2017; **241:** 80–90
Published online in Wiley Online Library
(wileyonlinelibrary.com) DOI: 10.1002/path.4831

ORIGINAL PAPER

Renal recruitment of B lymphocytes exacerbates tubulointerstitial fibrosis by promoting monocyte mobilization and infiltration after unilateral ureteral obstruction

Hui Han,[1,2] Jinzhou Zhu,[1] Yaqiong Wang,[3] Zhengbin Zhu,[1] Yanjia Chen,[1,2] Lin Lu,[1,2] Wei Jin,[1] Xiaoxiang Yan[1,2,*] and Ruiyan Zhang[1,2,*]

[1] *Department of Cardiology, Rui Jin Hospital, Shanghai Jiao Tong University School of Medicine, Shanghai, PR China*
[2] *Institute of Cardiovascular Diseases, Shanghai Jiao Tong University School of Medicine, Shanghai, PR China*
[3] *Department of Nephrology, Zhongshan Hospital, Shanghai Medical College, Fudan University, Shanghai, PR China*

**Correspondence to: R Zhang or X Yan, Department of Cardiology, Rui Jin Hospital, 197 Rui Jin 2nd Road, Shanghai 200025, PR China. E-mail: rjzhangruiyan@aliyun.com (Ruiyan Zhang); cardexyanxx@hotmail.com (Xiaoxiang Yan)*

Abstract

Renal fibrosis is a significant threat to public health globally. Diverse primary aetiologies eventually result in chronic kidney disease (CKD) and immune cells influence this process. The roles of monocytes/macrophages, T cells, and mast cells have been carefully examined, whilst only a few studies have focused on the effect of B cells. We investigated B-cell function in tubulointerstitial fibrosis induced by unilateral ureteral obstruction (UUO), using genetic B-cell-deficient μMT mice or CD20 antibody-mediated B-cell-depleted mice. Obstructed kidneys of μMT and anti-CD20-treated mice showed lower levels of monocyte/macrophage infiltration and collagen deposition compared to wild-type mice. Mechanistically, anti-CD20 attenuated UUO-induced alterations of renal tumour necrosis factor-α (TNF-α), vascular cell adhesion molecule 1 (VCAM-1) pro-inflammatory genes, and CC chemokine ligand-2 (CCL2) essential for monocyte recruitment; B cells were one of the main sources of CCL2 in post-UUO kidneys. Neutralization of CCL2 reduced monocyte/macrophage influx and fibrotic changes in obstructed kidneys. Therefore, early-stage accumulation of B cells in the kidney accelerated monocyte/macrophage mobilization and infiltration, aggravating the fibrosis resulting from acutely induced kidney nephropathy.

Keywords: B lymphocyte; fibrosis; CC chemokine ligand-2; unilateral ureteral obstruction

Received 29 March 2016; Revised 19 September 2016; Accepted 16 October 2016

No conflicts of interest were declared.

Introduction

Renal fibrosis, characterized by tubulointerstitial leukocyte infiltration, fibroblast proliferation, and increased matrix production, is the final common stage of progressive chronic kidney diseases (CKDs), irrespective of the initiating pathology [1,2]. Although CKD has become a major public health problem on a global scale, clinical strategies targeting renal fibrosis are rather disappointing [3–5]. In order to develop novel therapies for CKD patients, it is imperative to improve our understanding of the pathological process of renal fibrosis.

Infiltration of inflammatory cells, including T cells, monocytes/macrophages, dendritic cells, and mast cells, is a major cellular event in tubulointerstitial fibrosis [1]. Although inflammation is an essential part of host defence mechanisms following tissue injury, the infiltration of inflammatory cells serves as a potent driving force in the progression of renal fibrosis [2]. Despite the established correlation between sustained inflammation and fibrotic disease, the role of various inflammatory cells is highly complex. Infiltration and activation of macrophages, T cells, and dentritic cells contribute to fibrogenesis, while infiltrated mast cells tend to attenuate renal fibrosis induced by kidney injury [6–9]. To complicate matters, macrophages were also found to play an important role during the repair progress of the kidney when the cause of renal injury was resolved [10,11]. However, the role of B lymphocytes during the initiation and progression of renal fibrosis remains to be elucidated.

In the present study, by using genetic deficiency and anti-CD20-mediated depletion of B cells, we demonstrated that mature B lymphocytes critically contributed to tubulointerstitial fibrosis through regulation of the infiltration of monocytes into injured kidney after unilateral ureteral obstruction (UUO). In addition, other intervention approaches targeting the CC chemokine ligand-2/CC chemokine receptor-2 (CCL2/CCR2) pathway were also examined.

Materials and methods

Animals and study protocol

All mice were on a C57BL/6J background (male; studied at 6–8 weeks of age). Pathogen-free μMT mice

(B-cell-deficient) and their wild-type (WT) counterparts were kept in barrier units under a 12-h light/dark cycle. During the entire experiment, mice were provided with sterilized food and water *ad libitum*. After 1 week of accommodation, mice underwent surgical UUO or a sham operation, as previously described [12]. Briefly, the left proximal ureter was exposed and ligated at two separate locations in mice anaesthetized by sodium pentobarbital; sham-operated mice underwent exposure but not ligation of the left ureter. After surgery, flow cytometry (FCM) and histological assessments were performed at days 3 and 14, respectively.

For study 1, 1 h before surgery, WT mice were treated intraperitoneally with a previously validated mouse monoclonal CD20 antibody (200 μg per mouse) or isotype control rat IgG2b antibody. Thus, mice were divided into four groups: (1) sham-operated and isotype antibody-treated mice (isotype + sham, $n = 16$); (2) UUO model isotype antibody-treated mice (isotype + UUO, $n = 16$); (3) sham-operated and CD20 antibody-treated mice (anti-CD20 + sham, $n = 16$); and (4) UUO model and CD20 antibody-treated mice (anti-CD20 + UUO, $n = 16$). CD20 monoclonal antibody (clone 18B12) was kindly provided by Cherie Butts at Biogen Idec (Cambridge, MA, USA), and isotype control IgG antibody was obtained from eBioscience (San Diego, CA, USA; catalogue No 14-4321).

In study 2, mice were divided into four groups: (1) sham-operated WT mice (WT + sham, $n = 16$); (2) UUO model WT mice (WT + UUO, $n = 16$); (3) sham-operated μMT mice (μMT + sham, $n = 16$); and (4) UUO model μMT mice (μMT + UUO, $n = 16$). μMT mice were obtained from the Jackson Laboratory (Bar Harbor, ME, USA).

In study 3, CCL2 antibody (100 μg per mouse) or isotype control rat IgG2b antibody was injected intraperitoneally 1 h before the surgical procedure. Mice were divided into two groups: (1) UUO model isotype antibody-treated mice (isotype + UUO, $n = 8$) and (2) UUO model and anti-CCL2-treated mice (anti-CCL2 + UUO, $n = 8$). Anti-CCL2 and isotype control polyclonal hamster IgG antibody were purchased from Bio-X Cell (West Lebanon, NH, USA; catalogue Nos BE1085 and BE0091).

The study protocols were approved by the Committee on the Ethics of Animal Experiments of the Shanghai Jiao Tong University School of Medicine (permit No [2012]-86). Standards from the Guide for the Care and Use of Laboratory Animals (NIH Publication No 85-23, revised 1996) were followed.

Histological analysis

Masson's trichrome and Sirus red staining procedures were performed on 6 μm sections of paraffin-embedded kidneys to evaluate the severity of tubulointerstitial fibrosis. Interstitial collagen deposition relative to total interstitium was analysed quantitatively in ten randomly selected high-power fields of the cortical area per section, using Image Pro Plus 6.0 software on an Olympus Microsystems. The ratio of positively stained area to the total selected field was used to indicate the severity of tubulointerstitial fibrosis. In all experiments, glomerular areas were subtracted from the total cortical area.

Sections were used for immunohistochemistry analysis with the following antibodies: anti-CD45R (1:100), anti-F4/80 (1:200), anti-CD45 (1:100), and anti-CCL2 (1:50). After incubation with horseradish peroxidase (HRP)-conjugated secondary antibodies (1:100), sections were incubated with 3,3'-diaminobenzidine. For immunofluorescence, sections were incubated with anti-CD45R and anti-CCL2 antibodies and then with Alexa Fluor® 488- and 555-conjugated secondary antibodies (1:1000). Primary antibodies, including CD45R, F4/80, CD45, and CCL2 (catalogue Nos ab64100, ab6640, ab23910 and ab7202, respectively), were purchased from Abcam (Cambridge, MA, USA). Horseradish peroxidase (HRP)-, Alexa Fluor® 555-, and 488-conjugated secondary antibodies (catalogue Nos 31470, A-21428, and A-21208, respectively) were purchased from ThermoFisher (Waltham, MA, USA).

Flow cytometry

Peripheral blood was drawn via inferior vena cava puncture with heparin solution. Whole blood was lysed using FACS lysing solution (BD Biosciences, San José, USA) after immunofluorescence staining. Total leukocyte numbers were determined using trypan blue. Before kidney sample preparation and subsequent flow cytometry procedures, all anaesthetized mice underwent thorax opening and PBS perfusion. Briefly, the heart was exposed and the right atrium was cut open. A perfusion tube was inserted into the left ventricle and PBS perfusion was conducted until the effluent from the right atrium was clear and transparent. Spleens were collected, minced with fine scissors, and filtered through a 40 μm nylon mesh (BD Biosciences). The cell suspension was centrifuged at $400 \times g$ for 10 min at 4°C. Erythrocytes were lysed using lysing buffer according to the manufacturer's instructions (RBC Lysis Buffer; eBioscience, San Diego, CA, USA) and splenocytes were washed with FACS buffer. Renal cortex tissues were collected, minced with fine scissors, and placed into RPMI 1640 medium containing 40 mg/ml Liberase™ (Roche, Basel, Switzerland) and 8.5 U/ml DNase I (Roche) for 40 min at 37°C and then washed with serum-free RPMI 1640 medium. After erythrocyte lysis, cells were resuspended in FACS buffer.

To quantitatively analyse the number of leukocytes, the single cell suspensions were labelled with anti-CD45-FITC, anti-CD19-PE, anti-CD11b-Percp-cy5.5, and anti-Ly6-G-APC for 30 min in the dark at 4°C, and then washed with FACS buffer. All antibodies were used at a dilution of 1:100. Multicolour flow cytometry was performed on a flow cytometer (FACSAriaIII; BD Biosciences) and analysed using FlowJo software (Tree Star, Ashland, OR, USA). In addition, $CD19^+$ cells, $CD3^+$ cells, and $CD11b^+$ cells were sorted

for analysis of *Ccl2* mRNA levels. Anti-CD45-FITC (catalogue No 553079), anti-CD19-PE (catalogue No 557399), anti-CD11b-Percp-cy5.5 (catalogue No 561114), anti-Ly6-G-APC (catalogue No 560599), and anti-CD3-FITC (catalogue No 553062) were purchased from BD Biosciences.

Quantitative real-time polymerase chain reaction (qRT-PCR)

Total RNA was extracted using a Qiagen RNeasy kit according to the manufacturer's instructions. A total of 1 μg of RNA was reverse-transcribed into cDNA using a reverse transcription system (Promega, Madison, WI, USA). PCR amplification was performed with Power SYBR Green PCR Master Mix in a StepOne (Applied BioSystems, Foster City, CA, USA). The oligonucleotides used in quantitative real-time PCR analysis are listed in Table S1 of the supplementary material. Gene expression levels were normalized with β-actin and data were analysed with StepOne software v2.1 (Applied BioSystems).

Statistical analysis

Data were analysed using Prism 5.0 software (GraphPad Software Inc, San Diego, CA, USA) and SPSS 15.0 for Windows (SPSS Inc, Chicago, IL, USA), and are presented as mean ± standard deviation (SD). The significance of differences between two mean values was determined using unpaired *t*-tests. $p < 0.05$ was considered significant.

Results

Mature B lymphocytes are recruited to the injured kidney after UUO

To study infiltrating B lymphocytes in the process of renal fibrosis, we induced acute kidney injury in C57BL/6J mice by left urethral ligation and analysed single-cell suspensions of digested renal tissues by flow cytometry. Leukocytes and B lymphocytes accumulated in injured kidneys at the early stages of UUO. Compared with sham-operated mice, UUO mice had significantly increased infiltration of both $CD45^+$ leukocytes and $CD45^+CD19^+/CD45R^+$ B lymphocytes into the kidney 3 days after surgery (Figure 1A–D). In parallel, immunohistochemical staining for CD45 and CD45R was performed and confirmed these findings (Figure 1E–H).

Genetic deficiency and anti-CD20-mediated depletion of B cells protect obstructed kidneys from tubulointerstitial fibrosis after UUO

To examine the causal effect of B cells on UUO-induced renal fibrosis, anti-CD20 was used to deplete B lymphocytes [13]. A total of 99.93% and 80.32% of $CD45^+CD19^+$ B lymphocytes in the blood and spleen, respectively, were depleted at day 3 post-injection (see supplementary material, Figure S1). More importantly, B cells in the kidney were almost completely depleted with or without surgery (Figure 1B, D, F, H). Next, Masson's trichrome and Sirus red stains were used to assess the fibrotic changes in sham-operated and obstructed kidneys 2 weeks after surgery. Blue-stained (Masson's trichrome) and red-stained (Sirius red) areas were deemed collagen deposition. Collagen deposition was significantly higher in obstructed than in sham-operated kidneys (Figure 2). Notably, pretreatment with CD20 antibody protected the obstructed kidneys from fibrosis after UUO.

Because of their specific Igμ mutation and congenital B-cell deficiency, μMT mice were employed to further evaluate the protective effects of B-cell deficiency [14]. μMT mice lack $CD45^+CD19^+$ B lymphocytes (Figure 3A) and these mice were more resistant to fibrotic changes than C57BL/6J wild-type mice (Figure 3B–E).

B-cell depletion reduces macrophage infiltration into UUO kidneys

Influx of monocytes/macrophages into the renal interstitium is one of the typical features of acute kidney injury [15,16]. According to flow cytometry and immunohistochemical analysis of wild-type C57BL/6J mice, obstructed kidneys exhibited greater amounts of $CD11b^+Ly6\text{-}G^-/F4/80^+$ monocytic infiltrates than sham-operated mice (Figure 4). In mice pretreated with anti-CD20, infiltration of $CD11b^+Ly6\text{-}G^-/F4/80^+$ monocytes into the kidneys was suppressed (Figure 4B–E). Thus, these data indicated that B lymphocytes promote UUO-induced fibrosis through modulation of monocyte/macrophage mobilization and recruitment into injured kidney.

B-cell depletion alters chemotactic and pro-inflammatory responses after UUO

CC-family chemokines such as CCL2 and CCL7 play a vital role in the subsequent mobilization and relocation of inflammatory cells in response to acute injury. Thus, we examined the mRNA levels of *Ccl2* and *Ccl7* in cortical tissues by quantitative real-time PCR. *Ccl2* mRNA was elevated by UUO surgery and accompanied by the increased infiltration of B cells (Figure 5A and supplementary material, Figure S2). This effect of UUO was alleviated by pretreatment with anti-CD20. Although UUO resulted in up-regulation of *Ccl7* mRNA expression, anti-CD20 treatment failed to curb this alteration in the obstructed kidneys (Figure 5B, C).

To examine the main source of CCL2, $CD19^+$, $CD3^+$, and $CD11b^+$ cells were separately sorted from the kidneys at day 3 post-UUO. Compared with total cell samples from the UUO kidney, sorted $CD19^+$ cells had higher levels of *Ccl2* (Figure 5D). Immunofluorescent staining with both CD45R and CCL2 reinforced that

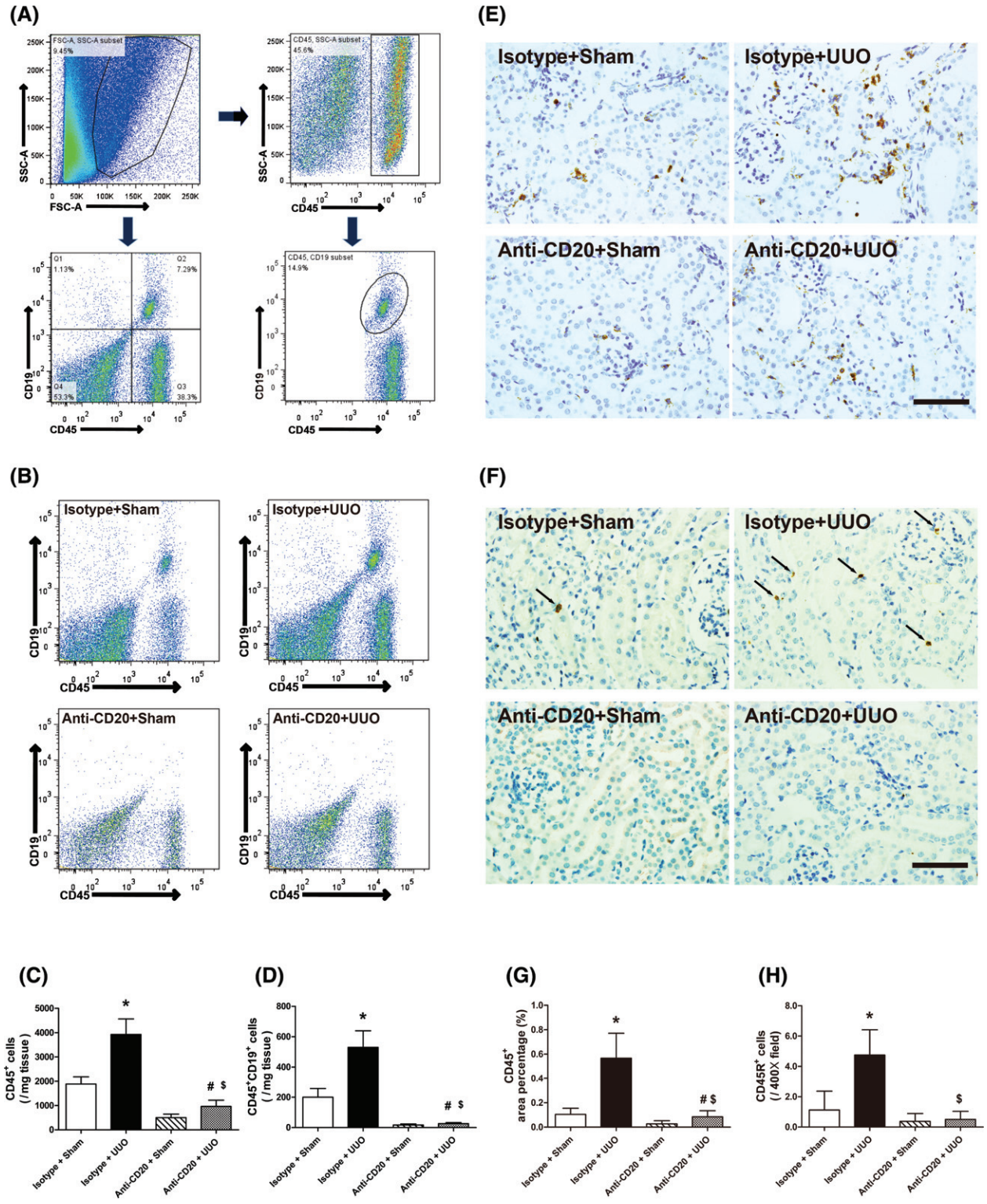

Figure 1. B-cell depletion reduces the infiltration of B lymphocytes into UUO kidney. (A) Gating strategy of flow cytometry analysis for infiltrating B lymphocytes in the kidneys. (B) Representative images of flow cytometry for renal $CD45^+CD19^+$ B lymphocytes in sham-operated and isotype antibody-treated (isotype + sham), UUO model isotype antibody-treated (isotype + UUO), sham-operated and CD20 antibody-treated (anti-CD20 + sham), and UUO model and CD20 antibody-treated (anti-CD20 + UUO) mice 3 days after surgery. (C, D) Quantitative analysis of renal infiltrating $CD45^+$ leukocytes and $CD45^+CD19^+$ B lymphocytes in isotype + sham, isotype + UUO, anti-CD20 + sham, and anti-CD20 + UUO mice 3 days after surgery. (E, F) Representative images and quantitative analysis of CD45 and CD45R staining in isotype + sham, isotype + UUO, anti-CD20 + sham, and anti-CD20 + UUO mice 3 days after surgery. Bar = 50 μm. $^*p < 0.05$ versus isotype + sham group; $^\#p < 0.05$ versus anti-CD20 + sham group; $^\$p < 0.05$ versus isotype + UUO group. Data are presented as mean ± SD ($n = 6–8$).

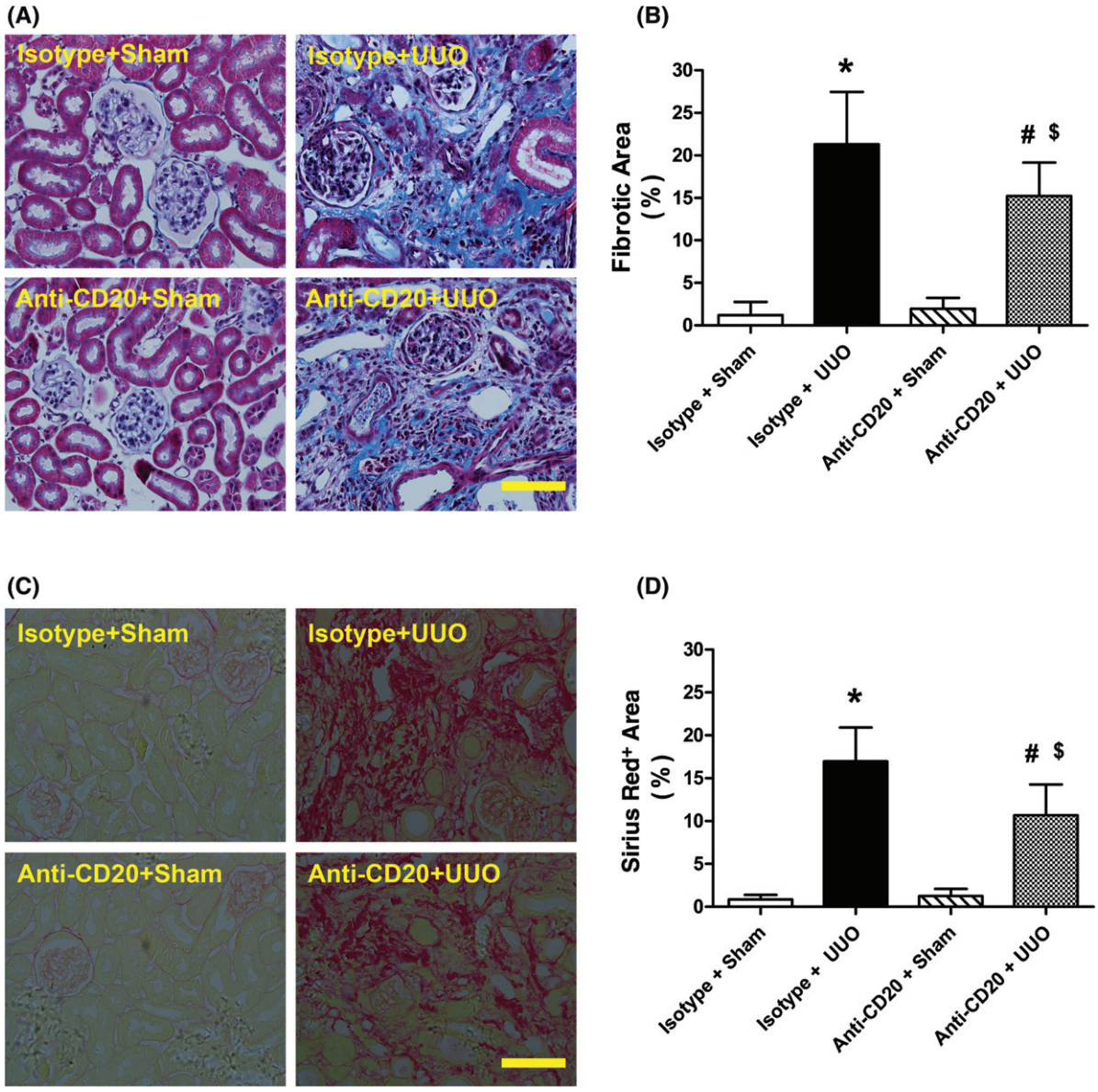

Figure 2. B-cell depletion ameliorates tubulointerstitial fibrosis after UUO. (A, B) Representative images and quantitative analysis of renal Masson's trichrome-stained sections in sham-operated and isotype antibody-treated (isotype + sham), UUO model isotype antibody-treated (isotype + UUO), sham-operated and anti-CD20 antibody-treated (anti-CD20 + sham), and UUO model and anti-CD20 antibody-treated (anti-CD20 + UUO) mice 2 weeks after surgery. Collagen is visible as the blue colour. Bar = 50 μm. (C, D) Representative images and quantitative analysis of Sirius red-stained renal sections in isotype + sham, isotype + UUO, anti-CD20 + sham, and anti-CD20 + UUO mice 2 weeks after surgery. Collagen is visible as the red stain. Bar = 50μm. $^{*}p < 0.05$ versus isotype + sham group; $^{\#}p < 0.05$ versus anti-CD20 + sham group; $^{\$}p < 0.05$ versus isotype + UUO group. Data are presented as mean ± SD ($n = 6–8$).

infiltrated B cells were a dominant source of renal CCL2 after UUO (Figure 5E).

Consistent with previous studies, UUO led to rapid inflammation in the affected kidneys [17]. We found that anti-CD20 antibody decreased the UUO-induced up-regulation of tumour necrosis factor-α (*Tnfa*) and vascular cell adhesion molecule 1 (*Vcam1*) mRNA levels (Figure 5F, G).

Neutralization of CCL2 attenuates monocytic infiltration and fibrotic changes after UUO

Next, we targeted the CCL2/CCR2 pathway by intraperitoneal injection of anti-CCL2 antibody. Flow cytometry and immunohistochemical analysis indicated that CCL2 antibody treatment inhibited the UUO-induced influx of $CD11b^{+}Ly6\text{-}G^{-}/F4/80^{+}$ monocytes into obstructed kidneys (Figure 6A–D). Finally, Masson's trichrome and Sirius red staining confirmed that CCL2 blockade antagonized fibrotic changes after UUO (Figure 6E–H).

Discussion

B lymphocytes play important roles in both innate and adaptive immune responses. Through antibody-dependent or antibody-independent mechanisms, they

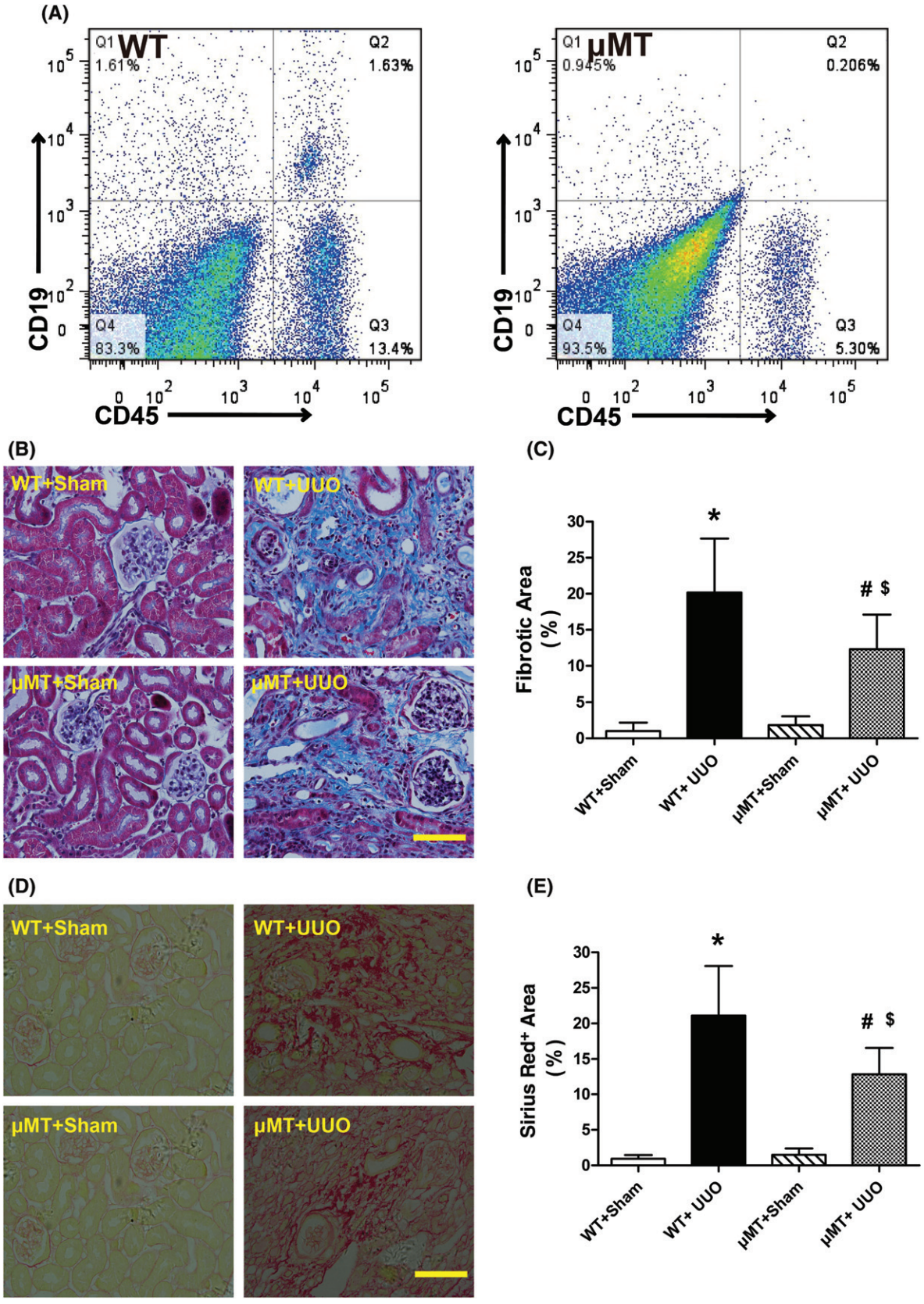

Figure 3. B-cell-deficient mice show decreased tubulointerstitial fibrosis after UUO. (A) Representative flow cytometry of renal $CD45^+CD19^+$ B lymphocytes in C57BL/6J (WT) and B-cell-deficient (μMT) mice. (B, C) Representative images and quantitative analysis of Masson's trichrome-stained sections in sham-operated WT (WT + sham), UUO model WT (WT + UUO), sham-operated μMT mice (μMT + sham), and UUO model μMT (μMT + UUO) mice 2 weeks after surgery. Collagen is visible as the blue stain. Bar = 50 μm. (D, E) Representative images and quantitative analysis of renal Sirius red-stained sections in WT + sham, WT + UUO, μMT + sham, and μMT + UUO mice 2 weeks after surgery. Collagen is visible as the red stain. Bar = 50 μm. $^*p < 0.05$ versus WT+sham group; $^\#p < 0.05$ versus μMT + sham group; $^\$p < 0.05$ versus WT + UUO group. Data are presented as mean ± SD ($n = 6–8$).

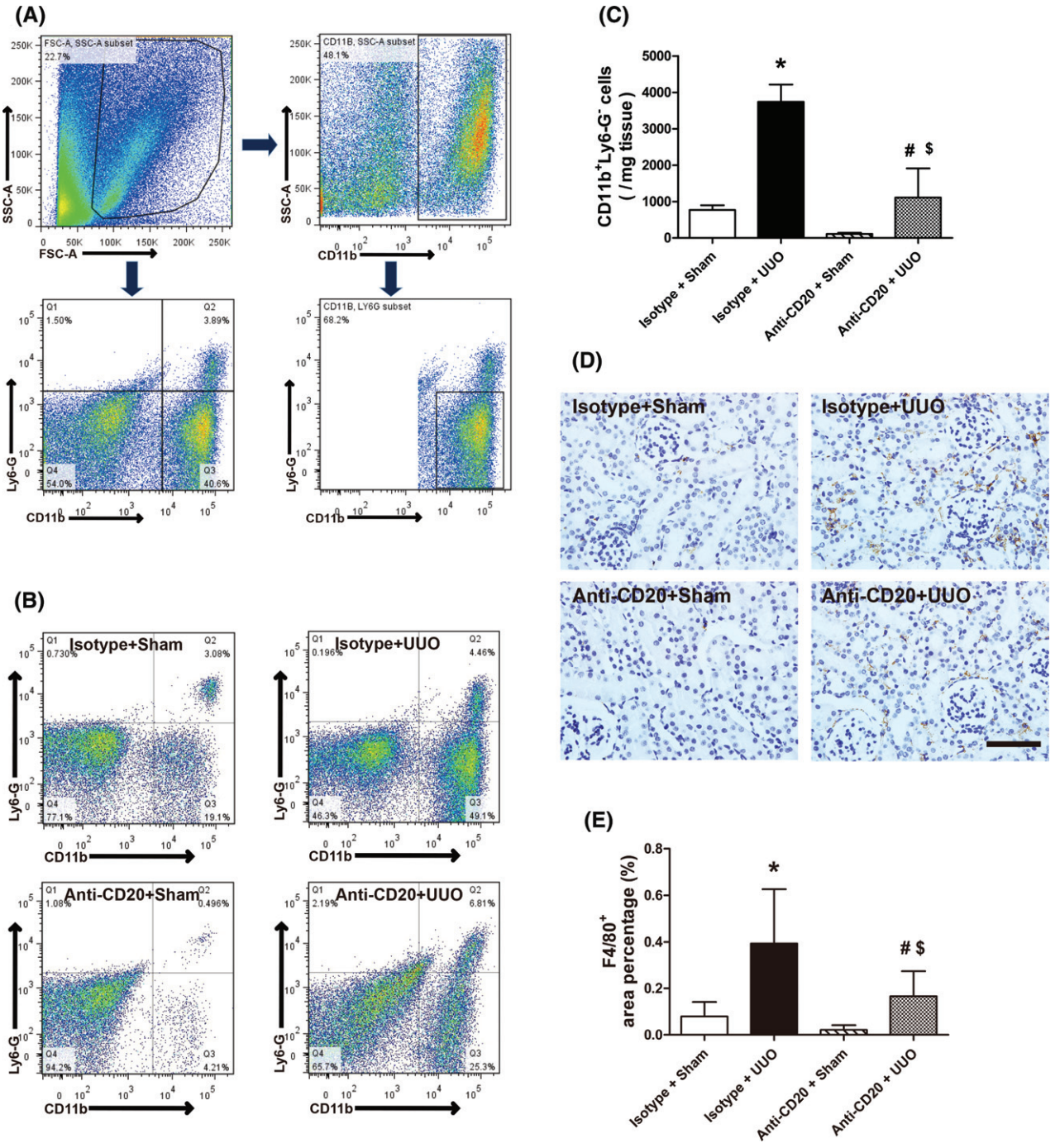

Figure 4. B-cell depletion reduces macrophage infiltration into UUO kidney. (A) Gating strategy of flow cytometry analysis for infiltrating macrophages in the kidneys. (B, C) Representative images and quantitative analysis of flow cytometry analysis for renal $CD11b^{+}Ly6\text{-}G^{-}$ macrophages in sham-operated and isotype antibody-treated (isotype + sham), UUO model and isotype antibody-treated (isotype + UUO), sham-operated and anti-CD20-treated (anti-CD20 + sham), and UUO model and anti-CD20-treated (anti-CD20 + UUO) mice 3 days after surgery. (D, E) Representative images and quantitative analysis of F4/80 staining in isotype + sham, isotype + UUO, anti-CD20 + sham, and anti-CD20 + UUO mice 3 days after surgery. Bar = 50 μm. $^{*}p < 0.05$ versus isotype + sham group; $^{\#}p < 0.05$ versus anti-CD20 + sham group; $^{\$}p < 0.05$ versus isotype + UUO group. Data are presented as mean ± SD ($n = 6–8$).

are rapidly activated and are involved in evoking subsequent inflammatory cascades [18–22]. To the best of our knowledge, our present study is the first to explore the triggering property of B lymphocytes during the mobilization and infiltration of monocytes/macrophages in the setting of UUO models.

Several signals are suspected of initiating inflammation in response to acute kidney injury, such as factors released or synthesized by injured cells, structural alterations in proteins or cell surfaces, and so forth [23]. Lymphocyte activation requires the recognition of these antigens via specific cell surface receptors [24,25]. After selective interaction within secondary lymphoid organs, B cells responsive to the same antigen migrate to the injury site. Once the immune response is initiated, cascade amplification will cause excess

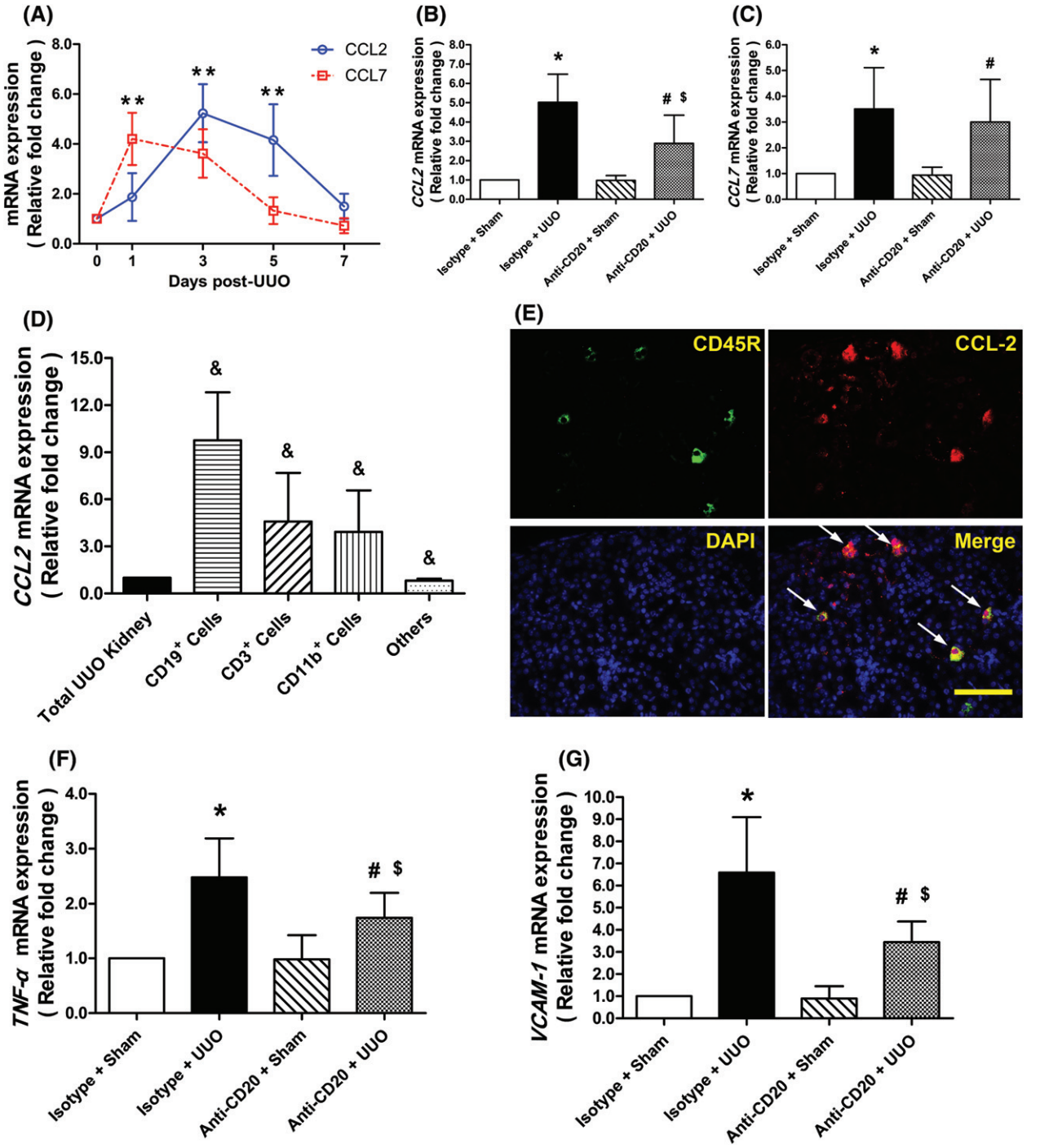

Figure 5. B-cell depletion alters chemotactic and pro-inflammatory responses after UUO. (A) Time course of mRNA expression of *Ccl2* and *Ccl7* after UUO surgery for wild-type mice. $^{**}p < 0.05$ versus day 0 ($n = 6$). (B, C) Quantitative RT-PCR analysis of *Ccl2* and C*cl7* mRNAs in kidneys from sham-operated and isotype antibody-treated (isotype + sham), UUO model isotype antibody-treated (isotype + UUO), sham-operated and anti-CD20-treated (anti-CD20 + sham), and UUO model anti-CD20-treated (anti-CD20 + UUO) mice 3 days after surgery. $^{*}p < 0.05$ versus isotype + sham group; $^{\#}p < 0.05$ versus anti-CD20 + sham group; $^{\$}p < 0.05$ versus isotype + UUO group ($n = 6–8$). (D) *Ccl2* mRNA levels in samples from the total UUO kidney, sorted $CD19^+$ cells, $CD3^+$ cells, and $CD11b^+$ cells, and the others 3 days after surgery. $^{\&}p < 0.05$ versus total UUO kidney ($n = 6$). (E) Immunofluorescence of kidney for CD45R, CCL2, and DAPI 3 days after surgery. Bar = 50 μm. (F, G) Quantitative RT-PCR analysis of *Tnfa* and *Vcam1* mRNA expression in the kidneys from isotype + sham, isotype + UUO, anti-CD20 + sham, and anti-CD20 + UUO mice 3 days after surgery. $^{*}p < 0.05$ versus isotype + sham group; $^{\#}p < 0.05$ versus anti-CD20 + sham group; $^{\$}p < 0.05$ versus isotype + UUO group ($n = 6–8$). Data are presented as means ± SD

leukocyte infiltration, which might persist into later stages of the disease. As a potent B-cell chemoattractant, B lymphocyte chemoattractant (BLC), whose expression is significantly increased in post-injury kidneys, is also involved in recruiting additional B cells [26]. It has been reported that overexpression of CXCR5, the receptor for BLC, was sufficient to overcome antigen-induced B-cell movement to the T-cell zone [27]. The present study did not examine the detailed signalling pathway for B-cell recruitment

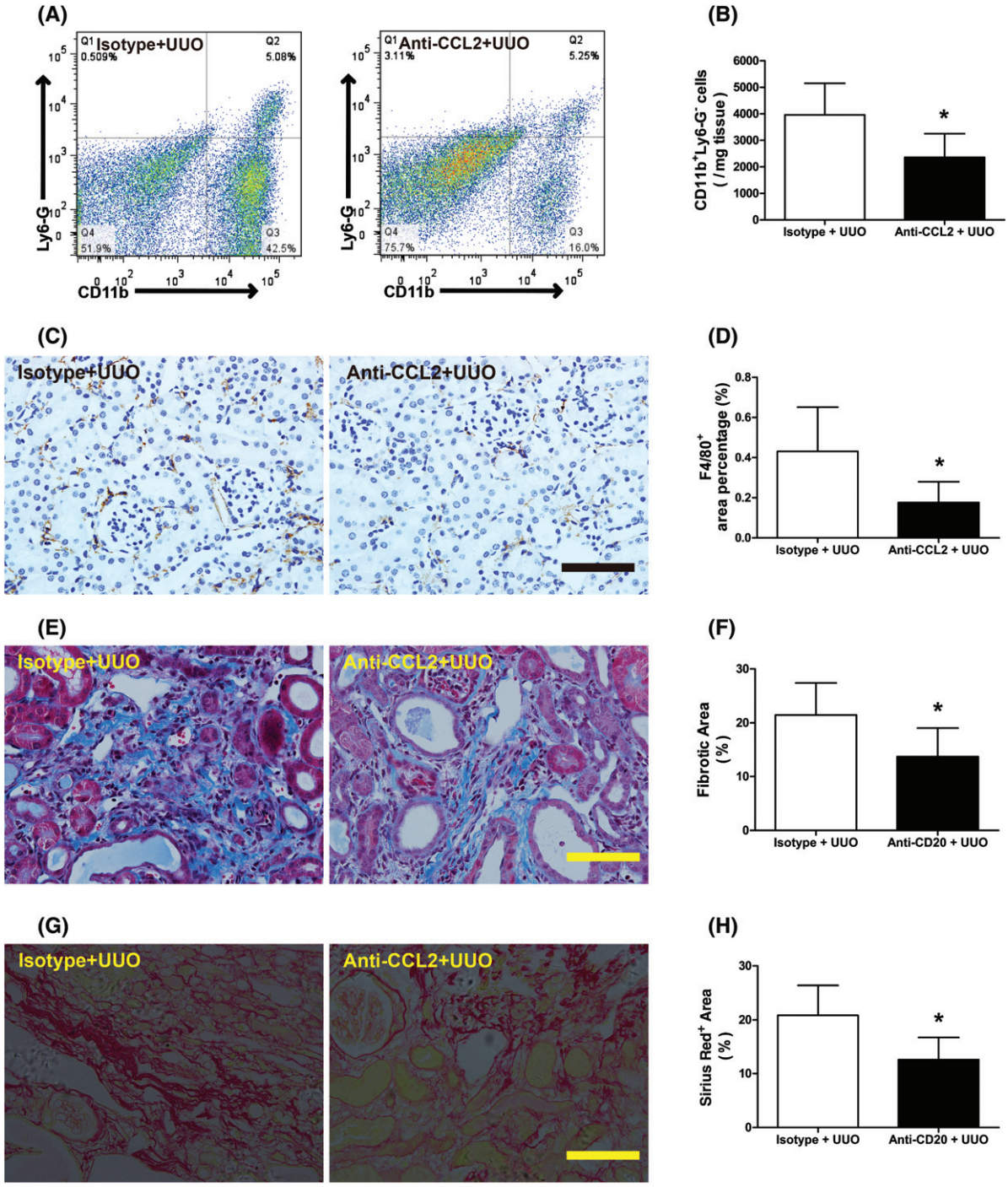

Figure 6. CCL2 depletion attenuates monocytic infiltration and fibrotic changes after UUO. (A, B) Representative flow cytometry and quantitative analysis of renal $CD11b^+Ly6\text{-}G^-$ macrophage staining in UUO model isotype antibody-treated (isotype + UUO) and UUO model anti-CCL2-treated (anti-CCL2 + UUO) mice 3 days after surgery. (C, D) Representative images and quantitative analysis of F4/80 staining in isotype + UUO and anti-CCL2 + UUO mice 2 weeks after surgery. (E, F) Representative images and quantitative analysis of Masson's trichrome-stained sections in isotype + UUO and anti-CCL2 + UUO mice 2 weeks after surgery. Collagen is visible as the blue stain. (G, H) Representative images and quantitative analysis of Sirius red-stained sections in isotype + UUO and anti-CCL2 + UUO mice 2 weeks after surgery. Collagen is visible as the blue stain. Bar = 50 μm. *$p < 0.05$ versus isotype + UUO group. Data are presented as means ± SD ($n = 6–8$).

towards the stressed kidney. However, it is possible that the above chemokines may be critically involved in this process, which needs further study.

As a typical model of renal fibrosis, UUO induces acute inflammation and monocytic infiltration in the renal tubulointerstitium [15]. The accumulated macrophages produce inflammatory cytokines, resulting in a detrimental cycle of tubulointerstitial fibrotic change. According to our experiments, a large number of B lymphocytes concomitantly infiltrate into the injured kidney during the early stages of this process, and B-cell depletion produced less macrophage infiltration and

reduced fibrotic area after UUO surgery. Our findings imply that B lymphocytes took part in the process of monocyte migration into the kidney tissue, which is deemed a key step during tubulointerstitial fibrosis.

How do B lymphocytes promote the influx of monocyte/macrophage into the kidney after UUO? As suggested in studies focused on immune cascades, there are several possible mechanisms, among which CCR2-mediated signals have received extensive attention [28,29]. Inflammatory monocytes express high levels of the chemokine receptor CCR2, and CCR2 and its ligands such as CCL2 and CCL7 were essential for rapid mobilization of inflammatory monocytes from their site of production (i.e. the bone marrow) to the blood, a necessary step for these cells to access injured tissues [16]. As two major ligands of CCR2, CCL2 and CCL7 were selectively examined in our study. Interestingly, B-cell-depleting strategies significantly down-regulated the mRNA levels of *Ccl2*, but not *Ccl7*, in UUO kidneys. Compared with infiltrated $CD3^+$ or $CD11b^+$ cells, $CD45R^+$ cells expressed high levels of *Ccl2* mRNA. In addition, immumofluorescent staining revealed that $CD45R^+$ cells produced a large amount of CCL2 in UUO kidney. These results imply that infiltrated B cells are at least one of the major producers of CCL2 in the injured kidneys, despite the minority of resident B cells.

Additionally, we selectively targeted the CCL2/CCR2 signalling pathway. Using a neutralizing antibody, we produced CCL2-depleted mice and, as expected, monocytic infiltrates into the UUO kidney were markedly curbed. Therefore, the CCL2/CCR2 pathway was involved in intrarenal B lymphocyte-promoted mobilization and relocation of monocytes/macrophages in injured renal tissues.

There are several limitations in our study. Firstly, infiltrated B lymphocytes were not further classified into subpopulations by the use of various clusters of differentiation. Secondly, we did not test our conclusion in the setting of other kidney disease models and clinical samples. Thirdly, further studies are needed to examine the possibility that B-cell depletion may also exert an effect on the proliferation of resident monocytes/macrophages, since we observed a reduction of renal $CD11b^+Ly6\text{-}G^-$ and $F4/80^+$ cells in sham mice receiving CD20 antibody.

In conclusion, B lymphocytes were rapidly recruited into the UUO kidney in the initiation stage of tubulointerstitial fibrosis, resulting in monocytic mobilization and infiltration through production of CCL2, and leading to pathological progression. Our study provides new insights into renal fibrosis and thus represents a potential therapeutic strategy for amelioration of the disease.

Acknowledgements

We would like to acknowledge Cherie Butts at Biogen Idec for generously providing monoclonal anti-CD20 antibody (clone 18B12). This study was supported by the National Natural Science Foundation of China (81570316, 81500196, and 81400362).

Author contribution statement

HH and XY wrote the main manuscript text and prepared all the figures and tables. RZ carried out the write-up of the manuscript and participated in research design. JZ, YW, ZZ, YC, LL, and WJ participated in data analysis. All the authors discussed and agreed on the results, and read and approved the final manuscript.

References

1. Zeisberg M, Neilson EG. Mechanisms of tubulointerstitial fibrosis. *J Am Soc Nephrol* 2010; **21:** 1819–1834.
2. Liu Y. Cellular and molecular mechanisms of renal fibrosis. *Nature Rev Nephrol* 2011; **7:** 684–696.
3. Tonelli M, Wiebe N, Culleton B, *et al.* Chronic kidney disease and mortality risk: a systematic review. *J Am Soc Nephrol* 2006; **17:** 2034–2047.
4. Coresh J, Selvin E, Stevens LA, *et al.* Prevalence of chronic kidney disease in the United States. *J Am Med Assoc* 2007; **298:** 2038–2047.
5. Sharma SK, Zou H, Togtokh A, *et al.* Burden of CKD, proteinuria, and cardiovascular risk among Chinese, Mongolian, and Nepalese participants in the International Society of Nephrology screening programs. *Am J Kidney Dis* 2010; **56:** 915–927.
6. Liu L, Kou P, Zeng Q, *et al.* CD4+ T lymphocytes, especially Th2 cells, contribute to the progress of renal fibrosis. *Am J Nephrol* 2012; **36:** 386–396.
7. Macconi D, Chiabrando C, Schiarea S, *et al.* Proteasomal processing of albumin by renal dendritic cells generates antigenic peptides. *J Am Soc Nephrol* 2009; **20:** 123–130.
8. Henderson NC, Mackinnon AC, Farnworth SL, *et al.* Galectin-3 expression and secretion links macrophages to the promotion of renal fibrosis. *Am J Pathol* 2008; **172:** 288–298.
9. Kim DH, Moon SO, Jung YJ, *et al.* Mast cells decrease renal fibrosis in unilateral ureteral obstruction. *Kidney Int* 2009; **75:** 1031–1038.
10. Vinuesa E, Hotter G, Jung M, *et al.* Macrophage involvement in the kidney repair phase after ischaemia/reperfusion injury. *J Pathol* 2008; **214:** 104–113.
11. Alikhan MA, Jones CV, Williams TM, *et al.* Colony-stimulating factor-1 promotes kidney growth and repair via alteration of macrophage responses. *Am J Pathol* 2011; **179:** 1243–1256.
12. Miyajima A, Chen J, Lawrence C, *et al.* Antibody to transforming growth factor-beta ameliorates tubular apoptosis in unilateral ureteral obstruction. *Kidney Int* 2000; **58:** 2301–2313.
13. Serreze DV, Chapman HD, Niens M, *et al.* Loss of intra-islet CD20 expression may complicate efficacy of B-cell-directed type 1 diabetes therapies. *Diabetes* 2011; **60:** 2914–2921.
14. Marino J, Paster JT, Trowell A, *et al.* B cell depletion with an anti-CD20 antibody enhances alloreactive memory T cell responses after transplantation. *Am J Transplant* 2016; **16:** 672–678.
15. Chevalier RL, Forbes MS, Thornhill BA. Ureteral obstruction as a model of renal interstitial fibrosis and obstructive nephropathy. *Kidney Int* 2009; **75:** 1145–1152.
16. Wang Y, Harris DC. Macrophages in renal disease. *J Am Soc Nephrol* 2011; **22:** 21–27.
17. Chuang ST, Kuo YH, Su MJ. KS370G, a caffeamide derivative, attenuates unilateral ureteral obstruction-induced renal fibrosis by the reduction of inflammation and oxidative stress in mice. *Eur J Pharmacol* 2015; **750:** 1–7.

18. Mizoguchi A, Bhan AK. A case for regulatory B cells. *J Immunol* 2006; **176:** 705–710.
19. Zouggari Y, Ait-Oufella H, Bonnin P, *et al.* B lymphocytes trigger monocyte mobilization and impair heart function after acute myocardial infarction. *Nature Med* 2013; **19:** 1273–1280.
20. Rauch PJ, Chudnovskiy A, Robbins CS, *et al.* Innate response activator B cells protect against microbial sepsis. *Science* 2012; **335:** 597–601.
21. Kelly-Scumpia KM, Scumpia PO, Weinstein JS, *et al.* B cells enhance early innate immune responses during bacterial sepsis. *J Exp Med* 2011; **208:** 1673–1682.
22. Burne-Taney MJ, Ascon DB, Daniels F, *et al.* B cell deficiency confers protection from renal ischemia reperfusion injury. *J Immunol* 2003; **171:** 3210–3215.
23. Thurman JM. Triggers of inflammation after renal ischemia/reperfusion. *Clin Immunol* 2007; **123:** 7–13.
24. Yuseff MI, Pierobon P, Reversat A, *et al.* How B cells capture, process and present antigens: a crucial role for cell polarity. *Nature Rev Immunol* 2013; **13:** 475–486.
25. Jones TB. Lymphocytes and autoimmunity after spinal cord injury. *Exp Neurol* 2014; **258:** 78–90.
26. Jang HR, Gandolfo MT, Ko GJ, *et al.* B cells limit repair after ischemic acute kidney injury. *J Am Soc Nephrol* 2010; **21:** 654–665.
27. Reif K, Ekland EH, Ohl L, *et al.* Balanced responsiveness to chemoattractants from adjacent zones determines B-cell position. *Nature* 2002; **416:** 94–99.
28. Wada T, Furuichi K, Sakai N, *et al.* Gene therapy via blockade of monocyte chemoattractant protein-1 for renal fibrosis. *J Am Soc Nephrol* 2004; **15:** 940–948.
29. Gonzalez J, Mouttalib S, Delage C, *et al.* Dual effect of chemokine CCL7/MCP-3 in the development of renal tubulointerstitial fibrosis. *Biochem Biophys Res Commun* 2013; **438:** 257–263.

SUPPLEMENTARY MATERIAL ONLINE

Supplementary figure legends

Figure S1. Anti-CD20 neutralizes B lymphocytes

Figure S2. B-cell kinetics after UUO surgery

Table S1. Real-time PCR primers